

Moving Target Indication with a Millimeter Wave Monopulse SAR

Maurice Rüegg
Remote Sensing Laboratories
University of Zürich
8057 Zürich, Switzerland
mrueegg@geo.unizh.ch

Manfred Hägelen
FGAN-FHR
Neuenahrer Strasse 20
53343 Wachtberg, Germany
m.haegelen@fgan.de

Erich Meier and Daniel Nüesch
Remote Sensing Laboratories
University of Zürich
8057 Zürich, Switzerland
{meier, nuesch}@geo.unizh.ch

Abstract—Synthetic aperture radar offers high resolution images of a static scene while moving objects are often smeared and displaced in azimuth. Ground moving target indication with a monopulse system makes it possible to correct the azimuth displacement and measure an accurate individual radial velocity component of moving targets via special processing techniques. The presented method requires the focused data from the sum and difference monopulse channels and is based upon specific deviations in the Doppler monopulse ratios due to object movement. For an experiment with the airborne millimeter wave radar system MEMHPIS and amplitude-comparison monopulse processing, frequency spectra and resulting accurate target velocities and positions are presented. They are used to verify the developed algorithms.

I. INTRODUCTION

The effects of smearing and displacement of moving targets in synthetic aperture radar (SAR) imagery have long been known and are discussed in detail in [1]. Ground moving target indication (GMTI) with SAR has been a widely explored field of interest ever since. Techniques for detection, position correction, refocusing, and velocity measurements of moving targets include the use of single- as well as multichannel SAR data. [2]–[4] give a good overview of some of them including multilooking, displaced phase center antenna (DPCA) processing, along-track interferometry (ATI), monopulse processing, and signal filtering by space time adaptive processing (STAP).

Monopulse processing for GMTI is often used tantamount to ATI in the SAR community [5]. We would like to make a distinction in that ATI refers to interferometry and the direct comparison of two or more received data records while monopulse or $\Sigma\Delta$ processing is a general term often used for tracking radar systems and always specified through a sum data signal and one or more isochronous difference data signals [6]. Monopulse processing looks at the complex ratios between these multiple signals and is thus well suited for GMTI.

Using a millimeter wave (mmW) SAR sensor for GMTI experiments has several advantages as well as drawbacks. Among the advantages are the relatively small size of the sensor antenna and hardware—suitable for application in small aircraft or drones—and a high GMTI sensitivity because of a short wavelength. The main drawbacks are a short signal range due to tropospheric attenuation, small target Doppler unambiguity, and extremely short baselines in interferometric applications that make ATI impractical as we will

see in Section II. Sections III and IV discuss the developed monopulse processing method and experimental results with the airborne mmW SAR MEMPHIS, respectively. We draw our conclusions in Section V.

II. MONOPULSE SAR

A monopulse radar has a sum signal Σ and multiple difference signals Δ . They are the result of two, four or more separate channels sending the same radio signal at the same time (hence the term monopulse), but receiving ground return echoes independently. While Σ is the sum signal of echoes from all channels, Δ is formed from the differences thereof. These differences in intensity as well as phase come from different viewing angles or, in the case of moving targets in SAR, from different Doppler frequency returns. Fig. 1 shows a schematic view of a monopulse system with four channels A, B, C, D . In a) the difference signal will be equal to zero, meaning a target at boresight with 0 Hz Doppler frequency, while b) and c) show targets that are displaced in either azimuth or azimuth and elevation (meaning a Doppler frequency different from zero for SAR).

If we assume a channel arrangement as in Fig. 1, we may express the sum and difference signals in azimuth and elevation as

$$\Sigma = A + B + C + D \quad (1)$$

$$\Delta_{az} = (A + C) - (B + D) \quad (2)$$

$$\Delta_{el} = (A + B) - (C + D) \quad (3)$$

Unlike a tracking radar, a SAR will only encounter targets displaced in azimuth and not in elevation. The elevation difference signal Δ_{el} does not play any important role and we will ignore it in the following. Hence, when referring to

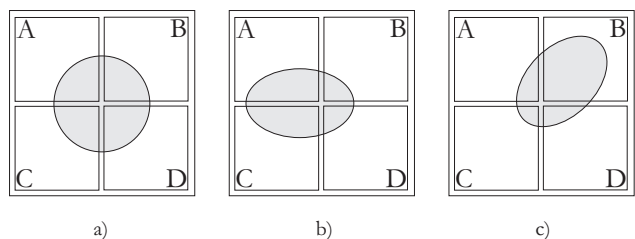


Fig. 1. Monopulse concept with a target seen by four independent receive channels A to D . In a) the target is at boresight, in b) and c) it is displaced.

Δ we will always mean the azimuth difference Δ_{az} . If we form the signal monopulse ratio defined as

$$\text{MPR} = \frac{\Delta}{\Sigma} \quad (4)$$

we will get zero for all boresight echoes of zero Doppler frequency, a distinct monopulse curve M from all other echoes as a function of Doppler frequency, and moving targets deviating from this curve.

A. Phase- and Amplitude-Comparison

There are two different kinds of monopulse radars.

- *amplitude-comparison monopulse* consists of multiple (horn) antennas in a parabolic reflector and a single lens bundling the individual signals and giving them a common phase center. The resulting look directions of the receive channels are squinted towards each other by an angle φ_0 .
- *phase-comparison monopulse* uses multiple separate antennas looking all in the same direction with a separation baseline B resulting in independent phase centers.

The two concepts are illustrated in Fig. 2. The idea of phase-comparison monopulse is commonly used in SAR interferometry applications. However, mmW SAR systems must rely on amplitude-comparison monopulse because the physical baseline B of phase-comparison monopulse with mmW SAR gets very small and hard to be practically realizable for GMTI applications. For example, experiments with radial target velocities v_r from 5 to 20 m/s at a carrier wavelength λ_c of 8 mm would result in a baseline of only 8 to 2 cm after the formula

$$B = \frac{\lambda_c v_s}{2 v_r} \quad (5)$$

and assuming an airborne SAR platform velocity in azimuth v_s of 100 m/s. (5) results under the assumption that an optimal phase difference between physical channels is $\lambda_c/2$. The time difference between the antenna phase centers at the same position is $t = B/v_s$ and during that time, a target will move a distance v_r/t equal to $\lambda_c/2$.

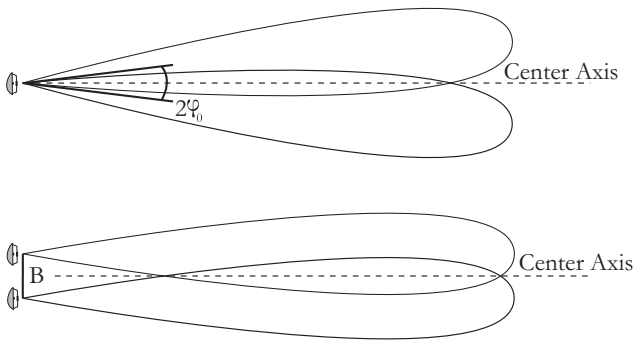


Fig. 2. Top: amplitude-comparison monopulse with one phase center and multiple squinted beams. Bottom: phase-comparison monopulse with two phase centers, parallel beams and a baseline.

B. The MEMPHIS SAR System

MEMPHIS is an experimental airborne mmW SAR developed by FGAN-FHR [7]. Its configuration permits an amplitude-comparison monopulse mode using a lens as described above to bundle the signals from four independent

horns arranged in a square. At the lens, the signals share a common phase center, but since the individual horns are separated locally from each other by a short distance, we will also get slight phase differences for moving targets in addition to intensity differences when looking at the monopulse ratios Δ/Σ .

The system operates simultaneously at both 35 and 94 GHz carrier frequency with a standard signal bandwidth of 200 MHz and a pulse repetition frequency (PRF) of 1700 Hz. For GMTI applications, the PRF may be increased to 3400 Hz when turning off the recording of one of the two carrier signals. Since the Doppler frequency of a target moving with radial velocity v_r is given as

$$f_d = \frac{2v_r}{\lambda_c} \quad (6)$$

we may receive unambiguous radial velocity measurements of 14.6 m/s at 3400 Hz PRF and 35 GHz if the target movement direction is known and ± 7.3 m/s otherwise. All higher radial target velocities are ambiguous. GMTI results from an experiment with MEMPHIS are shown in Section IV.

III. GMTI PROCESSING

A. Theory

While we have distinguished between amplitude- and phase-comparison monopulse methods in the previous Section II, the data processing approach may be the same for both. We do not look at amplitudes or phases but always at the complex ratios Δ/Σ or, to be more exact, we define the sum signal as

$$\Sigma = |\Sigma| \cdot e^{j\phi_\Sigma} \quad (7)$$

and the difference signal as

$$\Delta = |\Delta| \cdot e^{j\phi_\Delta} \quad (8)$$

to receive the complex monopulse ratios

$$\text{MPR} = \frac{\Delta}{\Sigma} = \frac{|\Delta|}{|\Sigma|} \cdot e^{j(\phi_\Delta - \phi_\Sigma)} \quad (9)$$

Specific to SAR, there are deviations from the general monopulse processing techniques described in chapter 7 of [6]. Most important of all, we look at the processed single look complex signals $S_c(r, \omega)$ in the range-Doppler domain instead of a direct analysis of signal amplitudes. The transformations from the received echo signal $s(t, z)$ at the antenna to the processed SAR image $s_c(r, z)$ and its equivalent in the range-Doppler domain, $S_c(r, \omega)$, is

$$s(t, z) \xrightarrow{\textcircled{1}} s_c(r, z) \xrightarrow{\textcircled{2}} S_c(r, \omega) \quad (10)$$

with t the fast time, r and z distances in range and azimuth and ω the Doppler frequency. $\textcircled{1}$ stands for the SAR processing of raw data to a single look complex image. $\textcircled{2}$ is the transformation into the range-Doppler domain given by the Fourier transform

$$S_c(r, \omega) = \int_{-\infty}^{\infty} s_c(r, z) e^{-j\omega z} dz \quad (11)$$

In the following, we calculate the monopulse ratio Δ/Σ for a SAR signal in the range-Doppler domain. Therefore,

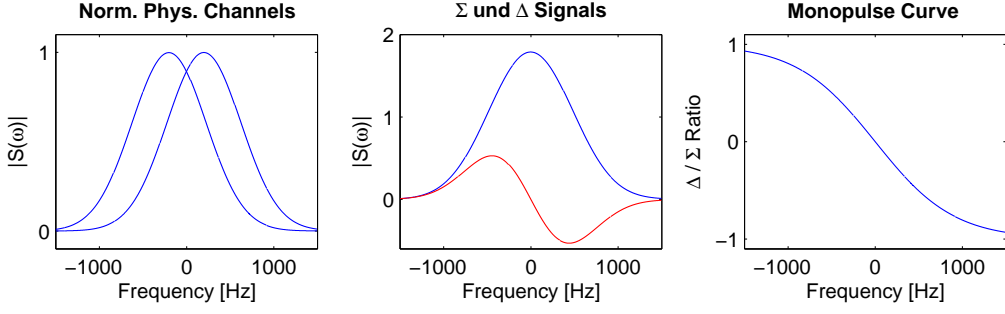


Fig. 3. The theoretical Doppler spectra of monopulse SAR — left: the normalized physical channels S_{c_1} and S_{c_2} , middle: the recorded monopulse signals of Σ and Δ , right: the monopulse curve M .

we do not assume a standard $\sin(x)/x$ radar backscattering intensity of the physical channels (see for example chapter 9 of [8]), but look at the Doppler frequency distribution at each range bin r as a standardized Gaussian distribution curve with a *half-power frequency* ω_p and a normalization constant $\nu = 1/\omega_p$. For simplicity reasons, we constrain ourselves to the amplitude of the complex spectra. We assume that the influence of the range r on the monopulse ratio is negligible for small image strips at large slant range distances. Thus, we define the image azimuth spectrum of the physical antenna channels independently from r as

$$S_{c_1}(\omega) = e^{-\nu^2(\omega+\omega_0)^2} \quad (12)$$

and

$$S_{c_2}(\omega) = e^{-\nu^2(\omega-\omega_0)^2} \quad (13)$$

ω_0 is the Doppler frequency shift of the channels resulting from the squinted antenna beams as in Fig. 2. We get the Σ und Δ signals

$$\begin{aligned} \Sigma(\omega) &= S_{c_1} + S_{c_2} \\ &= e^{-\nu^2(\omega+\omega_0)^2} + e^{-\nu^2(\omega-\omega_0)^2} \\ &= e^{-\nu^2\omega^2 - \nu^2\omega_0^2} \left(e^{2\nu^2\omega\omega_0} + e^{-2\nu^2\omega\omega_0} \right) \end{aligned} \quad (14)$$

and

$$\begin{aligned} \Delta(\omega) &= S_{c_1} - S_{c_2} \\ &= e^{-\nu^2(\omega+\omega_0)^2} - e^{-\nu^2(\omega-\omega_0)^2} \\ &= e^{-\nu^2\omega^2 - \nu^2\omega_0^2} \left(e^{2\nu^2\omega\omega_0} - e^{-2\nu^2\omega\omega_0} \right) \end{aligned} \quad (15)$$

Considering the properties of the hyperbolic functions $\sinh(x) = \frac{1}{2}(e^x - e^{-x})$ and $\cosh(x) = \frac{1}{2}(e^x + e^{-x})$ we get

$$\Sigma(\omega) = e^{-\nu^2(\omega^2+\omega_0^2)} \cdot 2 \cosh(2\nu^2\omega\omega_0) \quad (16)$$

and

$$\Delta(\omega) = e^{-\nu^2(\omega^2+\omega_0^2)} \cdot 2 \sinh(2\nu^2\omega\omega_0) \quad (17)$$

The monopulse curve of all Doppler frequencies from the static ground scene in a SAR may thus be described mathematically by a hyperbolic tangent as

$$M(\omega) = \frac{\Delta(\omega)}{\Sigma(\omega)} = \tanh(2\nu^2\omega\omega_0) \quad (18)$$

In Fig. 3, the physical channels given by (12) and (13) are plotted on the left while the sum and difference signals of (14) and (15) are shown in the center and the resulting monopulse

curve of (18) on the right. For this example, a total spectrum from -1500 to 1500 Hz was chosen with ω_p equal to 600 s^{-1} and ω_0 200 s^{-1} . Obviously, the slope of the monopulse curve depends on ω_0 and is thus directly related to the angle φ_0 between the physical channels. The larger φ_0 gets, the steeper the slope of Δ/Σ . This may be of an advantage when measuring very accurate target velocities with a small Doppler shift compared to the total signal spectrum. For a mmW SAR, however, the target Doppler shift will become large very fast because of the high carrier frequency, and a slight slope enables the exact measurement of a larger range of target velocities.

A moving target deviates from the monopulse curve of the static scene with the magnitude of deviation depending on the target's radial velocity component. This makes a moving target clearly discernible in the monopulse curve, regardless of whether the target's Doppler frequencies are inside or outside the clutter spectrum. Additionally, the monopulse curve of the static scene makes it possible to determine the Doppler shift of a target compared to the curve and therefore allows a correction of the azimuth displacement and estimation of the radial velocity.

B. Implementational Aspects

To be able to estimate an accurate monopulse curve $M(\omega)$ as theoretically defined in (18) from given sensor Σ and Δ signals and to identify moving targets therein, several steps are necessary including stochastic modeling of $M(\omega)$. All these steps are executed on blocks of data in the azimuth direction to avoid Doppler information from a too large sub-scene and multiple moving targets per range bin:

- 1) Because signal and SAR speckle noise may influence monopulse processing strongly, define an amplitude threshold and consider only Doppler frequency amplitudes in the sum signal $\Sigma(r, \omega)$ that are larger than the threshold.
- 2) Calculate and store the monopulse ratios $\text{MPR}(r, \omega) = \Delta(r, \omega)/\Sigma(r, \omega)$ over the complete Doppler spectrum for all range bins. Use only the real part of signals. The imaginary part may be considered for a phase correction later (see also chapter 3 of [6]).
- 3) Presuming independence of the monopulse ratio from range r , calculate the mean values of $\text{MPR}(\omega)$ at all frequencies.

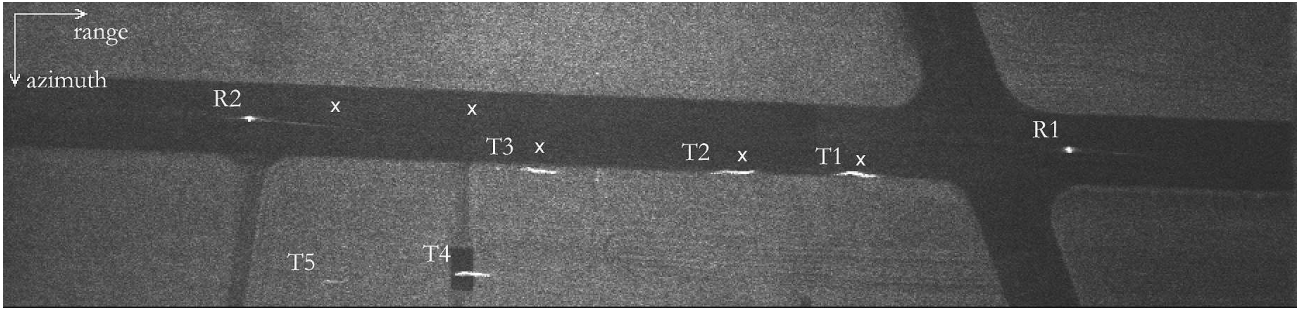


Fig. 4. MEMPHIS SAR image of the runway with moving targets T_1 to T_5 and static reflectors R_1 and R_2 . The true GPS positions of the moving targets are marked by x .

- 4) As shown in (18), the monopulse curve $M(\omega)$ has the form of a hyperbolic tangent. To fit a curve $M(\omega)$ through all values $\text{MPR}(\omega)$, assume a parameterization

$$M(\omega) = a \cdot \tanh(b\omega - c) \quad (19)$$

where a , b , and c are the free parameters.

- 5) Estimate a , b , and c through non-linear data modeling. A good technique is the Levenberg-Marquardt method in combination with singular value decomposition for the solution of the sets of linear equations (compare chapter 15 of [9]). Important for the method to work are well-guessed initial values of a , b , and c .
- 6) By estimating also the imaginary monopulse ratios and their monopulse curve $M_{im}(\omega)$, we may adjust the phase of all monopulse ratios through a multiplication of the complex Σ and Δ signals with $e^{-j\phi}$ where

$$\phi = \text{atan} \left(\frac{b_{im}}{b_{re}} \right) \quad (20)$$

and b_{re} , b_{im} are the b parameter of the real and imaginary monopulse curve.

- 7) Estimate the monopulse curve again, now with the phase-corrected ratios.
- 8) Define a monopulse threshold and ignore all ratios $\text{MPR}(r, \omega)$ that deviate less than the threshold from $M(\omega)$.
- 9) Determine the necessary frequency shift of all remaining signals presumed to be coming from moving targets. The frequency shifts may be directly translated into radial velocities v_r by (6), and an azimuth position correction in the image becomes possible.

Note that more than one target in the same range bin may be present if the block size of SAR images is set to be too large, complicating the algorithm. However, if it is too small, estimation of the monopulse curve $M(\omega)$ may be inaccurate.

IV. EXPERIMENTAL RESULTS

In June 2004, a GMTI experiment with the MEMPHIS SAR system was realized on the runway of the airfield in Emmen, Switzerland. Therein, five given targets were marked by Puch all-purpose vehicles with T_1 to T_3 at a nominally constant speed of 55 km/h and T_4 and T_5 at 35 km/h along the runway. Thus, they formed two independent small convoys. The front vehicle of either convoy (T_1 , T_4) was equipped with a corner reflector to increase signal reception of the SAR. The vehicles were moving down the runway with their exact positions and

velocities logged by GPS receivers at one second intervals. Post-measurement differential GPS processing was used to increase data accuracy. Two corner reflectors R_1 and R_2 were placed on the runway as well, serving as static reference targets.

The runway was imaged by MEMPHIS at 35 GHz, with 200 MHz signal bandwidth, a PRF of 3400 Hz, and a depression angle of 25° . Fig. 4 shows the 750 m wide Σ signal image with all targets and the corner reflectors. The targets were moving from left to right, away from the SAR sensor and are vertically displaced in the image. Note that the targets moving slower (T_4 , T_5) are actually displaced further away from their true position in the SAR image than the ones moving faster (T_1 - T_3). This happens because of the limited Doppler bandwidth (PRF ambiguities) implied by (6).

Monopulse GMTI processing as described in Section III-B yields the spectral results shown in Fig. 5. Given are the spectra for the static reflector R_1 and targets T_1 moving at 55 km/h and T_4 at 35 km/h. The calculated monopulse ratios at the range bin of the reflector at the top left of the figure correspond very well to the estimated monopulse curve. At the bottom left we see that no frequency remains in the spectrum after including a monopulse threshold. However, the target T_1 within the Doppler returns of the static environment (endoclipper) as well as the target T_4 outside of these returns (exoclipper) are clearly identified via monopulse processing. Their relative frequency shifts are easily detectable. Note that the monopulse curve estimated with the Levenberg-Marquardt method ranges from almost -2 to 2 because the PRF of 3400 Hz is ill-fitted to the actual ground return spectrum only about half as wide (compare the spectrum of the static reflector). Such a monopulse curve would not have been computable with only the theoretical curve of (18).

Fig. 6 shows the outcome in the time domain of our described monopulse algorithm. For orientation purposes, the airfield runway is outlined. The indicated targets appear in light gray and their calculated true ground positions in black. The resulting velocity components in slant range are listed in Table I and compared with calculated relative velocities between the sensor and the targets from differential GPS data. All targets are detected. Velocity estimates from the monopulse processing agree very well with GPS measurements with less than 3% deviation except for T_5 where velocity estimation and position correction are worse because of a too weak target signal intensity. Note that for all velocity

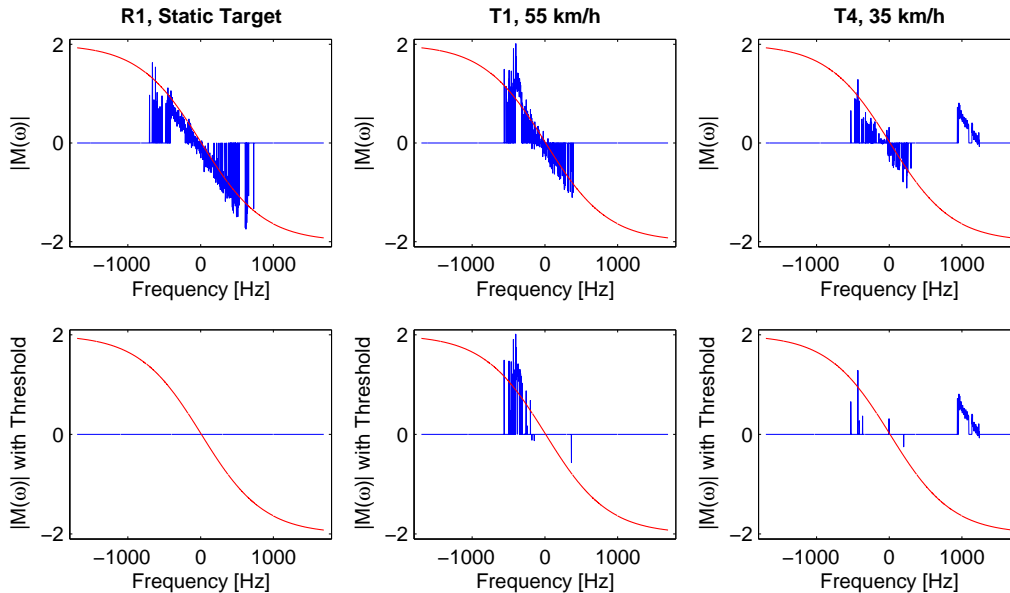


Fig. 5. Monopulse ratios before (top) and after (bottom) monopulse thresholding. Left: Monopulse ratios of a static reflector all fit on the monopulse curve. Middle: Indication of the endoclutler target T_1 . Right: Indication of the exoclutler target T_4 .

measurements the PRF ambiguity had to be considered. The faster target velocities are ambiguous by twice the PRF, the slower ones by once the PRF. This is also the reason why the slower targets T_4 and T_5 are displaced farther in the SAR image of Fig. 4.

TABLE I

ABSOLUTE NOMINAL VALUES AND MEASURED VELOCITIES OF MOVING TARGETS IN SLANT RANGE BY DIFFERENTIAL GPS AND BY THE MEMPHIS MONOPULSE SAR. THE NEGATIVE VALUES INDICATE A MOVEMENT AWAY FROM THE SAR.

Target	Nom. Velocity [km/h]	Radial GPS Velocity [km/h]	Radial SAR Velocity [km/h]
T_1	55	-51.2	-50.9
T_2	55	-50.8	-49.3
T_3	55	-50.3	-49.8
T_4	35	-33.6	-34.3
T_5	35	-30.2	-36.5

V. CONCLUSION

For mmW SAR systems, amplitude-comparison monopulse data recording is a very effective GMTI technique that solves the dilemma of extremely short baselines that make mmW ATI difficult to realize. It is a sound method with multiple channels sharing a single phase center. The basic concept is well-known from tracking radar applications and directly transferable to SAR GMTI scenarios.

Processing of monopulse data for SAR GMTI includes a mathematically complex nonlinear data modeling step to fit received and compressed signals to a stochastically determined hyperbolic tangent function in the range Doppler domain. Resulting deviations of moving targets from this function and thus from the static scene are well detectable and compensable, allowing for exact radial target velocity calculations and position shift corrections.

When calculating radial target velocities, a general problem for mmW SAR MTI are high Doppler frequency shifts from

the detected targets even at velocities of a few meters or less per second. PRF requirements for unambiguous velocity measurements are exceedingly high. Indication of targets, however, is very sensitive, and accurate position correction are possible also for ambiguous velocities.

Our experimental results obtained with the presented processing algorithm show the effectiveness of monopulse processing for SAR. Monopulse processing of the Δ/Σ Doppler signal ratios makes use of real as well as imaginary signal information. Velocity estimates and target displacement correction are accurate and fully automatically possible via monopulse ratio comparison of targets with our presented method of estimating a monopulse curve for the static scene. We could show that the theoretical hyperbolic tangent monopulse curve fits very well to measured static corner reflector data, giving proof to the practical application of our modeling approach.

ACKNOWLEDGMENT

We would like to thank the procurement and technology center of the Swiss Federal Department of Defence (*armasuisse*) and especially Peter Wellig for their wide support and cooperation.

REFERENCES

- [1] R. K. Raney, "Synthetic Aperture Imaging Radar and Moving Targets," *IEEE Transactions on Aerospace and Electronic Systems*, vol. 7, pp. 499–505, May 1971.
- [2] S. R. J. Axelsson, "Position Correction of Moving Targets in SAR-Imagery," *Proceedings of SPIE*, vol. 5236, pp. 80–92, Sept. 2003.
- [3] S. Chiu and C. E. Livingstone, "A Comparison of Displaced Phase Centre Antenna and Along-Track Interferometry Techniques for RADARSAT-2 Ground Moving Target Indication," *Canadian Journal of Remote Sensing*, vol. 31, no. 1, pp. 37–51, Feb. 2005.
- [4] J. H. G. Ender, "Space-time Processing for Multichannel Synthetic Aperture Radar," *Electronics and Communication Engineering Journal*, pp. 29–38, Feb. 1999.
- [5] M. Soumekh, "Moving Target Detection and Imaging Using an X-Band Along-Track Monopulse SAR," *IEEE Transactions on Aerospace and Electronic Systems*, vol. 38, no. 1, pp. 315–333, Jan. 2002.

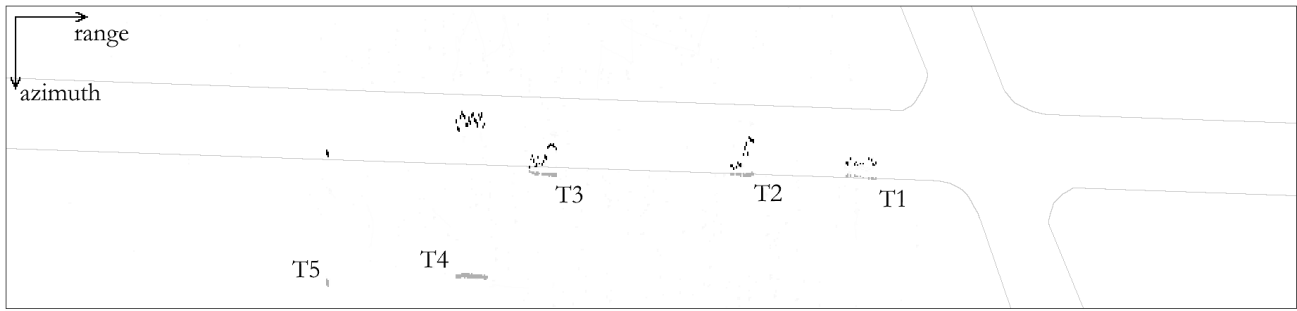


Fig. 6. Monopulse processed SAR image of Fig. 4. Reflectors R_1 and R_2 have vanished. All targets are identified and their position corrected. For ease of interpretation, the runway edges have been outlined in the image.

[6] S. M. Sherman, *Monopulse Principles and Techniques*. Boston: Artech House Publishers, 1984.

[7] H. Schimpf, H. Essen, S. Böhmendorff, and T. Brehm, "MEMPHIS - A Fully Polarimetric Experimental Radar," *Proceedings of the IEEE International Geoscience and Remote Sensing Symposium IGARSS*, vol. 3, pp. 1714–1716, June 2002.

[8] B. R. Mahafza and A. Z. Elsherbeni, *Matlab Simulations for Radar System Design*. Boca Raton: Chapman & Hall / CRC, 2004.

[9] W. H. Press, B. P. Flannery, S. A. Teukolsky, and W. T. Vetterling, *Numerical Recipes in C: The Art of Scientific Computing, Second Edition*. Cambridge: Cambridge University Press, 1992.